CHAPTER IV

CATALYTIC OXIDATION OF NAPHTHALENE OVER CeO_2-ZrO_2 MIXED OXIDE CATALYSTS*

4.1 Abstract

In this study, the vapor phase catalytic oxidation of naphthalene was studied over CeO_2-ZrO_2 mixed oxide catalysts prepared via urea hydrolysis. The $Ce_{0.75}Zr_{0.25}O_2$ solid solution catalyst exhibits the highest activity for the naphthalene oxidation, and the extent of the activity is related to its degree of reducibility. Moreover, the $Ce_{0.75}Zr_{0.25}O_2$ catalyst shows a high selectivity towards CO_2 with no formation of by-products. Kinetic studies show that the reaction rates strongly depend on both naphthalene and oxygen concentrations. From the power law model, the reaction orders of naphthalene and oxygen were estimated to equally be 0.5. The Mars-van Krevelen mechanism is in good agreement with the experimental results. The estimated activation energy of the reaction is ca. 90 kJ/mol.

4.2 Introduction

Catalytic combustion has been proved to be an effective method for the abatement of volatile organic compounds (VOCs) such as alkanes, aromatics, oxygenated and halogenated hydrocarbons, including polycyclic aromatic hydrocarbons (PAHs). (Choudhary *et al.*, 2002; Gélin *et al.*, 2002; Zhang *et al.*, 2003). Precious metal catalysts supported on alumina have been demonstrated as the most active catalysts for the destruction of these obnoxious compounds with the high cost burden. Some of the most active catalysts are Pt/Al_2O_3 and $Pt/V/Al_2O_3$ (Zhang *et al.*, 2003; Carnö *et al.*, 1996; Shie *et al.*, 2005; Ndifor *et al.*, 2006). Alternatively, metal oxide catalysts such as MnO_x, Fe_2O_3, CoO_x, ZnO, TiO_2 and CeO_2 were introduced (García *et al.*, 2006). Among a wide range of metal oxides, CeO_2 was reported to have an excellent activity for the oxidation of naphthalene with a high

---

naphthalene adsorption capacity (García *et al.*, 2006). A combination of high surface area and high redox properties seems to be important factors for the catalytic oxidation of naphthalene (García *et al.*, 2006; Ndifor *et al.*, 2007).

It is known that the substitution of Ce^{4+} with Zr^{4+} in the lattice of CeO_2 leads to improvement in its oxygen storage capacity, redox property, and thermal resistance. With the unique properties and high oxygen storage capacity, $Ce_{1-x}Zr_xO_2$ mixed oxides have been utilized for the oxidation of hydrocarbons and the removal of post-combustion pollutants (Thammachart *et al.*, 2001; Pengpanich *et al.*, 2002; Pengpanich *et al.*, 2006). However, the catalytic performance of several systems for the catalytic combustion of alkanes and mono-aromatic compounds cannot be directly extrapolated to predict the activities for the total oxidation of PAHs (García *et al.*, 2006; Garcia *et al.*, 2006). Moreover, the catalytic combustion of PAHs, particular for naphthalene, has rarely been investigated and reported in literature.

Since, the search for more active and cost-effective catalysts based on metal oxides for the complete oxidation of PAHs remains essential, therefore the present study aims at a better understanding of the naphthalene oxidation activities over $Ce_{1-x}Zr_xO_2$ mixed oxide catalysts. The kinetic analysis over the most active catalyst and reaction kinetic expressions were purposed.

4.3 Experimental

4.3.1 Catalyst Preparation and Characterizations

In this study, CeO_2-ZrO_2 mixed oxide catalysts were prepared via urea hydrolysis. Cerium nitrate ($Ce(NO_3)_3 \cdot 6H_2O$ (99.0%), Fluka), and zirconium oxychloride ($ZrOCl_2 \cdot 8H_2O$ (99.0%), Fluka) were used as sources of Ce and Zr, respectively. Different formulas were achieved with varying different Ce/Zr ratios. The synthesis procedure and characteristics of catalysts has been reported elsewhere (Pengpanich *et al.*, 2002).

4.3.2 Activity Tests and Kinetic Studies

Catalytic activity tests for the naphthalene oxidation were carried out in a differential fixed-bed quartz tube reactor in which its dimensions were reported

elsewhere (Pengpanich *et al.*, 2002). Typically, 50 mg of a catalyst was packed between the layers of quartz wool. The catalyst bed temperature was monitored and controlled by a Shinko temperature controller equipped with two type-K thermocouples inserted at the catalyst bed and next to the reactor. A total flow rate of 200 ml/min gas mixtures containing 200 ppmv (part per million by volume) of naphthalene, 10% oxygen and balance of helium was used. Exit gases were chromatographically analyzed for CO, CO_2 and naphthalene using a Shimadzu GC 8A equipped with a TCD detector and a Shimadzu GC 17A equipped with an FID detector.

The kinetic studies were carried out in the same system as mentioned earlier at the temperatures of 543, 573, 603 and 633 K. The concentrations of the reactant gases were varied between 100 and 1200 ppmv for naphthalene, 1 and 10% for oxygen, and balance of helium. The kinetic data were obtained using the initial rate method.

4.4 Results and Discussion

4.4.1 Catalytic Activities for Naphthalene Oxidation

Figure 4.1 shows the light-off temperatures for the naphthalene oxidation over $Ce_{1-x}Zr_xO_2$ mixed oxide catalysts. A higher activity is indicated by a lower temperature for 50% conversion of naphthalene (T50%). Regardless of the mixed oxide used, CO_2 and H_2O are the only products observed. The results show that the catalytic activity of the mixed oxide catalysts is higher than that of ZrO_2. In addition, the catalytic activity of the mixed oxides decreases with an increase in the Zr loading, regardless of the surface areas, which are in same range (ca. 120 m^2/g). $Ce_{0.75}Zr_{0.25}O_2$ was found to exhibit the highest activity for the oxidation of naphthalene, resulted from the fact that $Ce_{0.75}Zr_{0.25}O_2$ possesses the highest reducibility as shown in Figure 4.2. The sequence of reducibility of the CeO_2-ZrO_2 mixed oxide catalysts follows in the order: $Ce_{0.75}Zr_{0.25}O_2 \geq Ce_{0.50}Zr_{0.50}O_2 > Ce_{0.25}Zr_{0.75}O_2$, which is the same order as its catalytic activity. This suggests that the degree of reducibility be significantly affected by the addition of Zr content greater than 0.5. Therefore, we can claim that the catalytic activity is related to the redox

properties of the mixed oxide catalysts. This finding is in similar manners of CO and CH_4 oxidation (Thammachart *et al.*, 2001; Pengpanich *et al.*, 2002).

4.4.2 Kinetic Studies

The kinetic studies of naphthalene oxidation were carried out on the highest catalytic activity material, $Ce_{0.75}Zr_{0.25}O_2$, at reaction temperatures ranging from 543 to 633 K. In order to ensure the elimination of mass and heat transfer effects, the initial rate data were collected at the linear range conversions of less than 20% in all cases and conformed to Mears and Prater-Weisz criteria (Mears, 1971; Weisz and Prater, 1954).

The effect of the variation of naphthalene and oxygen partial pressure on the rate of reaction is shown in Figure 4.3. It was found that the reaction rate of the oxidation increases with the increase in the partial pressures of both naphthalene and oxygen. It should be noted that, with excess oxygen in the system, the overall reaction rate still depends on the oxygen partial pressure. This finding is similar to that reported for the case of hydrocarbons and aromatic compounds oxidation over mixed oxide catalysts (Trimm and Irshad, 1970; Haber andTurek, 2000). However, it is apparent that the reaction rate of naphthalene decomposition over 1% $Pt/\gamma-Al_2O_3$ became insensitive to the concentration of oxygen once the reaction temperature exceeds 413 K (Zhang *et al.*, 2003). This is due to the fact that dissociated oxygen adsorbed more strongly on the Pt surface than on naphthalene (Zhang *et al.*, 2003; Neyestanaki and Lindfors, 1998). From our results, it seems that the catalytic oxidation of naphthalene over $Ce_{0.75}Zr_{0.25}O_2$ depends primarily on the oxygen adsorption rate.
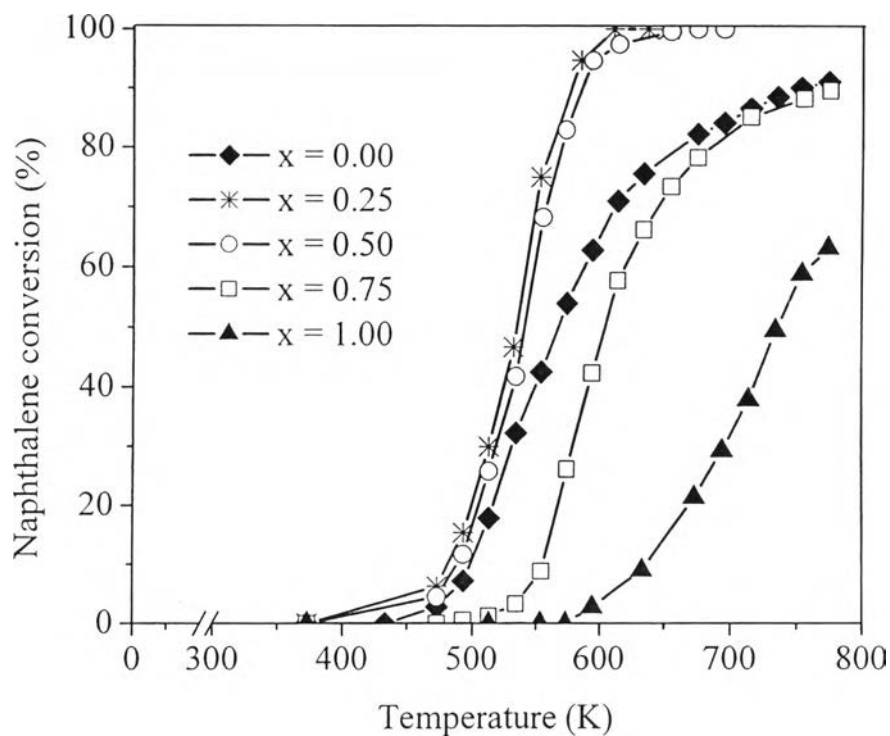
Figure 4.1 Light-off curves for naphthalene oxidation over $Ce_{1-x}Zr_xO_2$ mixed oxide catalysts; with a gas mixture composed of 200 ppmv $C_{10}H_8$, 10% O_2 and balance He.

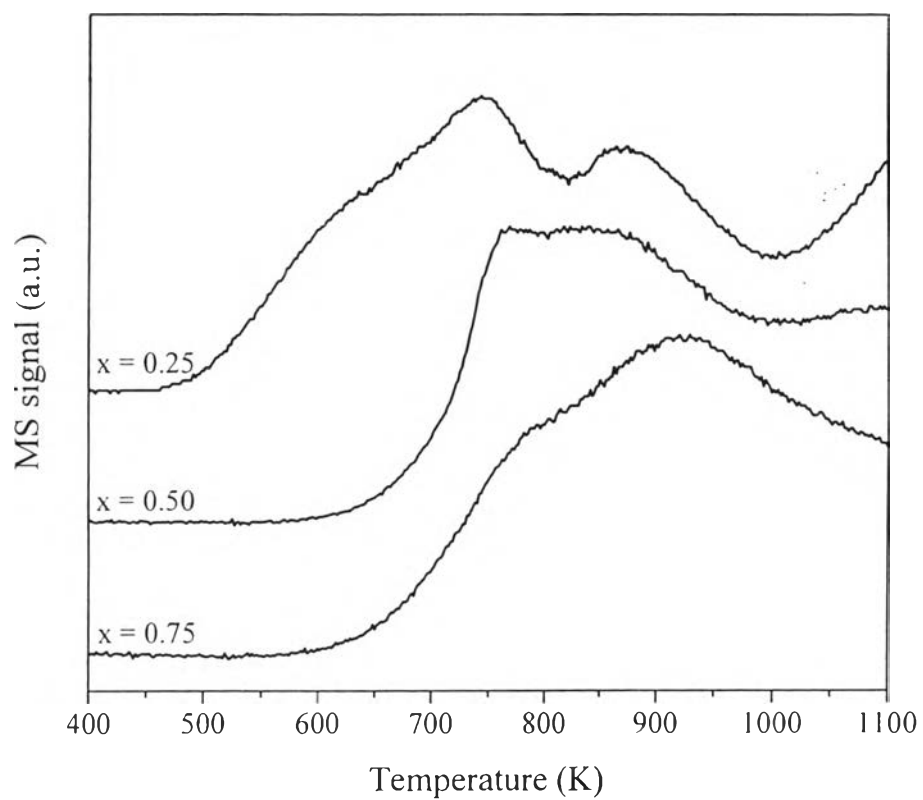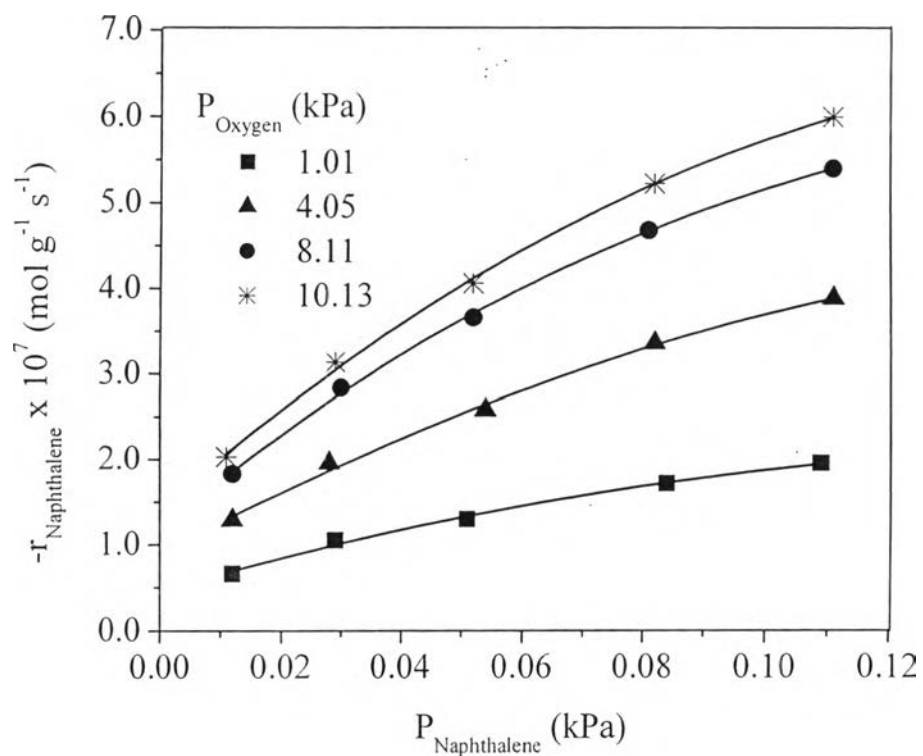**Figure 4.2** CO-TPR profiles of the $Ce_{1-x}Zr_xO_2$ mixed oxide catalysts.

Figure 4.3 Experimental reaction rate ($r_{Naphthalene}$) vs. $P_{Naphthalene}$ at different P_{Oxygen} values at 543 K for the $Ce_{0.75}Zr_{0.25}O_2$ mixed oxide catalyst.

The reaction order of the catalyst was determined by using a power law model. It was found that the reaction orders of both naphthalene and oxygen are equally about 0.49±0.01 (ca. 0.50) with the correlation coefficient of 0.998. This result conforms to the dependency of the partial pressure of the reactants on the reaction rate, generally about 0.5 orders for naphthalene and oxygen. The calculated apparent activation energy obtained from the Arrhenius plot (Figure 4.4 (A)) for this model is 89.36 ±0.14 kJ/mol. This value is significantly lower than those reported for the naphthalene oxidation over V_2O_5 (121.80 kJ/mol) (D'Alessandro et $al.$, 1956) and Pt/γ-Al_2O_3 (149.97 kJ/mol) (Shie et $al.$, 2005).

Surface reaction mechanisms were proposed based on the classical Langmuir-Hinshelwood model, Eley-Rideal model and Mars-van Krevelen model (Masel, 1996) for the catalytic oxidation of naphthalene in our study. The details of each model are summarized in Table 4.1.

By performing a multi-linear regression analysis, the results are reported in Table 4.2. The Eley-Rideal mechanisms with a difference in the adsorption step of oxygen (expressions 1 and 2) appear to little correlate with the experimental data.

Although the Langmuir-Hinshelwood models (expressions 3 and 4) yield high values of R^2, 0.994 and 0.972, respectively, they did not obey the van't Hoff's law implying that the equilibrium constants obtained were less meaningful. A similar characteristic was reported for the oxidation of o-xylene over a vanadium oxide catalyst (Juusola et $al.$, 1970).

Hence, it seems that only does the Mars-van Krevelen rate expression best describe the catalytic oxidation of naphthalene over the $Ce_{0.75}Zr_{0.25}O_2$ catalyst ($R^2 = 0.996$);

$$-r_{Nap} = \frac{k_r k_o p_{Nap} p_{O_2}}{k_o p_{O_2} + n k_r p_{Nap}}, \tag{4.1}$$

where n is the stoichiometric coefficient for the total oxidation reaction (mol O_2/mol naphthalene), p_{Nap} and p_{O_2} denote the partial pressures of naphthalene and oxygen,

respectively, k_o is the kinetic constant for the non-equilibrium adsorption of oxygen on the catalyst surface, and k_r is the kinetic constant for the reaction between chemisorbed oxygen and naphthalene. The result is consistent with that reported for the oxidation of aromatic compounds over noble metal and metal oxide catalysts (Young and Greene, 1977; Barresi and Baldi, 1994; Grabowski, 2006).

It should be pointed out that the activities of these mixed oxide catalysts followed the reducibility of the catalysts, suggesting that the naphthalene oxidation over mixed oxide catalysts occur via the Mars-van Krevelen mechanism. The result is in agreement with that reported for the kinetic mechanism of the toluene oxidation over metallic mixed oxide catalysts (Rodrigues, 2007).

The kinetic constants for the Mars-van Krevelen model are graphically shown in Figure 4.4 (B) and the activation energies of reduction and oxidation steps of the naphthalene oxidation calculated based on this surface reaction mechanism are similarly obtained about 91.95±0.24 and 89.10±0.31 kJ/mol, respectively. However, the pre-exponential factor of the oxidation step (2.66±0.01 mol/kPa·g·s) is much lower than that of the reduction step ($1.41\pm0.01\times10^4$ mol/kPa·g·s), suggesting that the oxidation step is a rate-determining step. Similar phenomena were also found in the cases of CH_4, C_6H_{12}, C_6H_6, C_7H_8, and benzo (a) pyrene oxidation over noble and metal oxide catalysts (Juusola et $al.$, 1970; Young and Greene, 1977; Ordóñez et $al.$, 2002; Bahlawane, 2006).
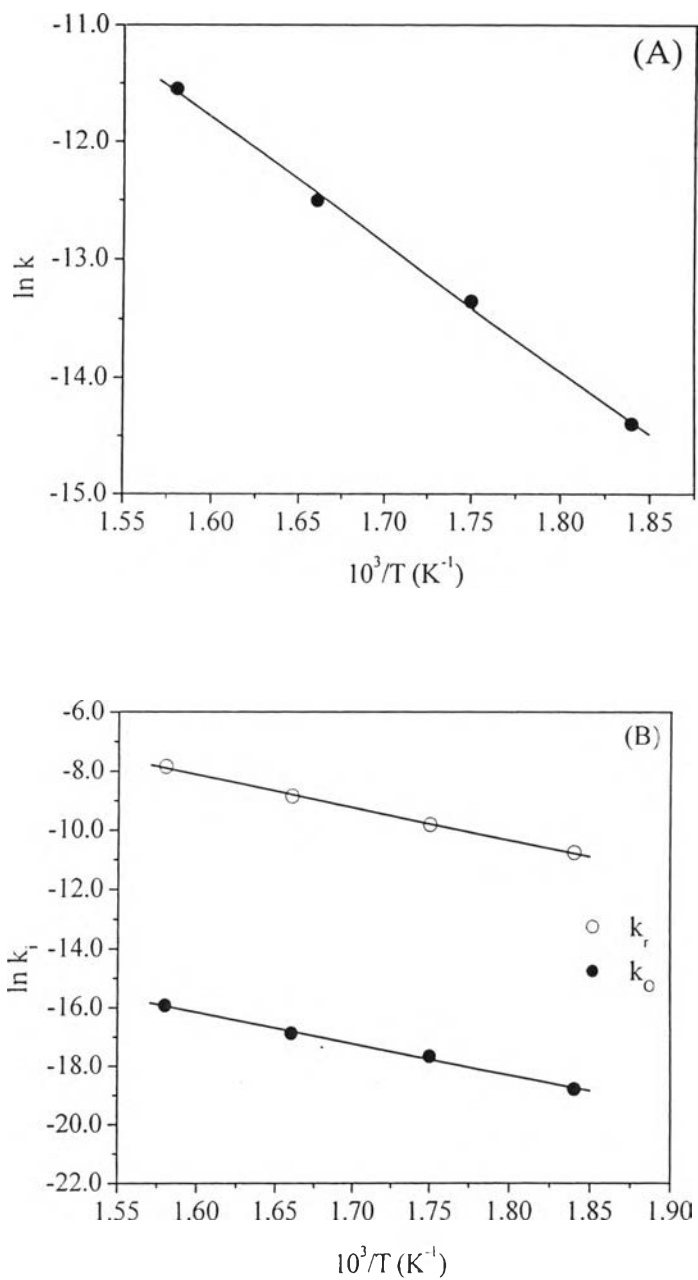
Figure 4.4 Arrhenius plots of reaction rate constants for the catalytic oxidation of naphthalene over $Ce_{0.75}Zr_{0.25}O_2$ mixed oxide catalyst by: (A) power law model; (B) Mars-van Krevelen model.

Table 4.1 Kinetic models tested in fitting the naphthalene oxidation process

Expression	Assumptions	Reaction mechanism	Rate determining step	Rate expression
1	Eley-Rideal model: equilibrium molecular adsorption of oxygen reacted with gas phase naphthalene	$O_2 + X \xleftrightarrow{K_1} O_2 - X$ $Nap + O_2 - X \xrightarrow{k_2} product - X$ $product - X \xrightarrow{k_3} product + X$	$Nap + O_2 - X \xrightarrow{k_2} product - X$	$-r_{Nap} = \dfrac{k_2 K_1 p_{O_2} p_{Nap}}{1 + K_1 p_{O_2}}$
2	Eley-Rideal model: equilibrium dissociative adsorption of oxygen reacted with gas phase naphthalene	$O_2 + 2X \xleftrightarrow{K_1} 2O - X$ $Nap + O - X \xrightarrow{k_2} product - X$ $product - X \xrightarrow{k_3} product + X$	$Nap + O - X \xrightarrow{k_2} product - X$	$-r_{Nap} = \dfrac{k_2 K_1^{1/2} p_{O_2}^{1/2} p_{Nap}}{1 + \left(K_1 p_{O_2}\right)^{1/2}}$
3	Langmuir-Hinshelwood model: equilibrium molecular adsorption of both naphthalene and oxygen, with reaction occurring between adsorbed reactants	$O_2 + X \xleftrightarrow{K_1} O_2 - X$ $Nap + X \xleftrightarrow{K_2} Nap - X$ $Nap - X + O_2 - X \xrightarrow{k_3} product - X + X$ $product - X \xrightarrow{k_4} product + X$	$O_2 + X \xleftrightarrow{K_1} O_2 - X$ $Nap + X \xleftrightarrow{K_2} Nap - X$ $Nap - X + O_2 - X \xrightarrow{k_3} product - X + X$	$-r_{Nap} = \dfrac{k_1 p_{O_2}}{1 + K_2 p_{Nap}}$ $-r_{Nap} = \dfrac{k_2 p_{Nap}}{1 + K_1 p_{O_2}}$ $-r_{Nap} = \dfrac{k_3 K_1 K_2 p_{O_2} p_{Nap}}{\left(1 + K_1 p_{O_2} + K_2 p_{Nap}\right)^2}$
4	Langmuir-Hinshelwood model: equilibrium dissociative adsorption of oxygen and molecular adsorption of naphthalene, with reaction occurring between adsorbed reactants	$O_2 + 2X \xleftrightarrow{K_1} 2O - X$ $Nap + X \xleftrightarrow{K_2} Nap - X$ $Nap - X + O - X \xrightarrow{k_3} product - X + X$ $product - X \xrightarrow{k_4} product + X$	$O_2 + 2X \xleftrightarrow{K_1} 2O - X$ $Nap + X \xleftrightarrow{K_2} Nap - X$ $Nap - X + O - X \xrightarrow{k_3} product - X + X$	$-r_{Nap} = \dfrac{k_1 p_{O_2}}{\left(1 + K_2 p_{Nap}\right)^2}$ $-r_{Nap} = \dfrac{k_2 p_{Nap}}{1 + \left(K_1 p_{O_2}\right)^{1/2}}$ $-r_{Nap} = \dfrac{k_3 K_1^{1/2} K_2 p_{O_2}^{1/2} p_{Nap}}{\left(1 + \left(K_1 p_{O_2}\right)^{1/2} + K_2 p_{Nap}\right)^2}$
5	Mars-van Krevelen model: the reaction takes place through alternative oxidation and reduction of the catalyst surface	$Nap + oxidized\ catalyst \xrightarrow{k_r}$ $product + reduced\ catalyst$ $reduced\ catalyst + oxygen \xrightarrow{k_o}$ $oxidized\ catalyst$		$-r_{Nap} = \dfrac{k_r k_o p_{Nap} p_{O_2}}{k_o p_{O_2} + n k_r p_{Nap}}$

Table 4.2 Values of the rate parameters obtained for naphthalene oxidation over $Ce_{0.75}Zr_{0.25}O_2$ mixed oxide catalyst

Expression	Rate expression	Rate parameter	Temperature (K)				R^2
			543	573	603	633	
1	$-r_{Nap} = \dfrac{k_2 K_1 p_{O_2} p_{Nap}}{1 + K_1 p_{O_2}}$	K_1 (kPa⁻¹)	0.274±0.111	0.383±0.311	0.313±0.113	0.313±0.133	0.678
		$k_2 \times 10^5$ (mol kPa⁻¹ g⁻¹ s⁻¹)	1.067±0.353	2.472±1.086	6.859±2.805	16.789±7.766	
2	$-r_{Nap} = \dfrac{k_2 K_1^{1/2} p_{O_2}^{1/2} p_{Nap}}{1 + \left(K_1 p_{O_2}\right)^{1/2}}$	$K_1 \times 10^4$ (kPa⁻¹)	1.734±0.437	45.751±15.958	0.785±0.229	23.423±7.505	0.062
		$k_2 \times 10^4$ (mol kPa⁻¹ g⁻¹ s⁻¹)	2.001±1.777	1.176±0.836	20.355±19.135	9.910±7.527	
3	$-r_{Nap} = \dfrac{k_1 p_{O_2}}{1 + K_2 p_{Nap}}$	K_2 (kPa⁻¹)	-6.563±3.027	-6.137±4.082	-7.116±4.038	-6.700±4.088	0.623
		$k_1 \times 10^7$ (mol kPa⁻¹ g⁻¹ s⁻¹)	0.308±0.044	0.970±0.198	2.303±0.404	6.000±1.156	
	$-r_{Nap} = \dfrac{k_2 p_{Nap}}{1 + K_1 p_{O_2}}$	K_1 (kPa⁻¹)	-0.073±0.029	-0.082±0.043	-0.087±0.044	-0.083±0.039	0.686
		$k_2 \times 10^5$ (mol kPa⁻¹ g⁻¹ s⁻¹)	0.275±0.036	0.748±0.118	1.794±0.283	4.652±0.666	
	$-r_{Nap} = \dfrac{k_3 K_1 K_2 p_{O_2} p_{Nap}}{\left(1 + K_1 p_{O_2} + K_2 p_{Nap}\right)^2}$	K_1 (kPa⁻¹)	0.169±0.005	0.180±0.001	0.196±0.003	0.194±0.003	0.994
		K_2 (kPa⁻¹)	15.418±0.318	13.481±0.072	15.509±0.061	15.381±0.149	
		$k_3 \times 10^5$ (mol g⁻¹ s⁻¹)	0.380±0.053	1.087±0.116	2.357±0.279	6.153±0.808	
4	$-r_{Nap} = \dfrac{k_1 p_{O_2}}{\left(1 + K_2 p_{Nap}\right)^2}$	K_1 (kPa⁻¹)	-4.050±1.583	-3.624±1.912	-4.382±2.023	-4.029±2.031	0.623
		$k_2 \times 10^7$ (mol kPa⁻¹ g⁻¹ s⁻¹)	0.317±0.055	1.036±0.239	2.372±0.503	6.307±1.456	
	$-r_{Nap} = \dfrac{k_2 p_{Nap}}{1 + \left(K_1 p_{O_2}\right)^{1/2}}$	K_2 (kPa⁻¹)	0.061±0.031	0.066±0.041	0.072±0.044	0.066±0.039	0.714
		$k_1 \times 10^6$ (mol kPa⁻¹ g⁻¹ s⁻¹)	2.110±0.303	5.811±1.080	13.770±2.514	36.420±6.268	
	$-r_{Nap} = \dfrac{k_3 K_1^{1/2} K_2 p_{O_2}^{1/2} p_{Nap}}{\left(1 + \left(K_1 p_{O_2}\right)^{1/2} + K_2 p_{Nap}\right)^2}$	$K_1 \times 10^5$ (kPa⁻¹)	7.175±0.400	28.003±0.181	3.949±0.242	1.141±0.073	0.972
		K_2 (kPa⁻¹)	7.683±0.476	7.040±0.532	8.696±0.568	8.491±0.527	
		$k_3 \times 10^4$ (mol g⁻¹ s⁻¹)	0.868±0.045	1.198±0.076	7.456±0.402	36.140±2.061	
5	$-r_{Nap} = \dfrac{k_r k_o p_{Nap} p_{O_2}}{k_o p_{O_2} + n k_r p_{Nap}}$	$k_r \times 10^5$ (mol kPa⁻¹ g⁻¹ s⁻¹)	2.137±0.037	5.481±0.095	14.353±0.510	38.976±1.681	0.996
		$k_o \times 10^8$ (mol kPa⁻¹ g⁻¹ s⁻¹)	0.697±0.023	2.143±0.101	4.710±0.229	12.091±0.558	

4.5 Conclusions

In conclusion, the catalytic activity for the naphthalene oxidation over CeO_2-ZrO_2 mixed oxide catalysts is directly relative to the catalyst redox properties. The optimal composition of the CeO_2-ZrO_2 mixed oxide catalyst that gives the highest activity is attained with $Ce_{0.75}Zr_{0.25}O_2$. Based on kinetic studies, the reaction rate of catalytic oxidation of naphthalene depends on both the naphthalene and oxygen concentrations. The reaction mechanism can be expressed by the Mars-van Krevelen mechanism, with oxygen of the metallic oxides acting as the active oxygen, being consumed during the naphthalene oxidation and restored by oxygen from the gas-phase. The oxidation step is identified as the rate-determining step with its activation energy of ca. 90 kJ/mol.

4.6 Acknowledgements

4.7 References

Bahlawane, N. (2006) Kinetics of methane combustion over CVD-made cobalt oxide catalysts. Applied Catalysis B: Environmental, 67, 168-176.

Barresi, A.A., Baldi, G. (1994) Deep catalytic oxidation of aromatic hydrocarbon mixtures: Reciprocal inhibition effects and kinetics. Industrial & Engineering Chemistry Research, 33, 2964-2974.

Carnö, J., Berg, M., Järås, S. (1996) Catalytic abatement of emissions from small-scale combustion of wood: A comparison of the catalytic effect in model and real flue gases. Fuel, 75, 959-965.

Choudhary, T.V., Banerjee, S., Choudhary, V.R. (2002) Catalysts for combustion of methane and lower alkanes. Applied Catalysis A: General, 234, 1-23.

D'Alessandro, A.F., Farkas, A. (1956) The kinetics of the catalytic oxidation of naphthalene. Journal of Colloid Science, 11, 653-670.

Garcia, T., Solsona, B., Cazorla-Amorós, D., Linares-Solano, A., Taylor, S.H. (2006) Total oxidation of volatile organic compounds by vanadium promoted palladium-titania catalysts: Comparison of aromatic and polyaromatic compounds. Applied Catalysis B: Environmental, 62, 66-76.

García, T., Solsona, B., Taylor, S.H. (2006) Naphthalene total oxidation over metal oxide catalysts. Applied Catalysis B: Environmental, 66, 92-99.

Gélin, P., Primet, M. (2002) Complete oxidation of methane at low temperature over noble metal based catalysts: a review. Applied Catalysis B: Environmental, 39, 1-37.

Grabowski, R. (2006) Kinetics of oxidative dehydrogenation of C_2-C_3 alkanes on oxide catalysts. Catalysis Reviews: Science and Engineering, 48, 199-268.

Haber, J., Turek, W. (2000) Kinetic studies as a method to differentiate between oxygen species involved in the oxidation of propene. Journal of Catalysis, 190, 320-326.

Juusola, J.A., Mann, R.F., Downie, J., 1970. The kinetics of the vapor-phase oxidation of o-xylene over a vanadium oxide catalyst. Journal of Catalysis, 17, 106-113.

Masel, R.I. (1996) Principles of Adsorption and Reaction on Solid Surfaces. John Wiley & Sons, New York.

Mears, D.E. (1971) Tests for transport limitations in experimental catalytic reactors. Industrial and Engineering Chemistry Product Research and Development, 10, 541-547.

Ndifor, E.N., Garcia, T., Solsona, B., Taylor, S.H. (2006) Naphthalene oxidation over vanadium-modified Pt catalysts supported on γ-Al_2O_3. Catalysis Letter, 110, 125-128.

Ndifor, E.N., Garcia, T., Solsona, B., Taylor, S.H. (2007) Influence of preparation conditions of nano-crystalline ceria catalysts on the total oxidation of

naphthalene, a model polycyclic aromatic hydrocarbon. Applied Catalysis B: Environmental, 76,248-256.

Neyestanaki, A.K., Lindfors, L.-E. (1998) Catalytic clean-up of emissions from small-scale combustion of biofuels. Fuel, 77, 1727-1734.

Ordóñez, S., Bello, L., Sastre, H., Rosal, R., Díez, F.V. (2002) Kinetics of the deep oxidation of benzene, toluene, n-hexane and their binary mixtures over a platinum on γ-alumina catalyst. Applied Catalysis B: Environmental, 38, 139-149.

Pengpanich, S., Meeyoo, V., Risksomboon, T., Bunyakiat, K. (2002) Catalytic oxidation of methane over CeO_2-ZrO_2 mixed oxide solid solution catalysts prepared via urea hydrolysis. Applied Catalysis A: General, 234, 221-233.

Pengpanich, S., Meeyoo, V., Risksomboon, T., Schwank, J. (2006) Hydrogen production from partial oxidation of iso-octane over $Ni/CeO_{0.75}Zr_{0.25}O_2$ and Ni/β''-Al_2O_3 catalysts. Applied Catalysis A: General, 302, 133-139.

Rodrigues, A.C.C. (2007) Metallic mixed oxides (Pt, Mn, or Cr) as catalysts for the gas-phase toluene oxidation. Catalysis Communications, 8, 1227-1231.

Shie, J.-L., Chang, C.-Y., Chen, J.-H., Tsai, W.-T., Chen, Y.-H., Chiou, C.-S., Chang, C.-F., 2005. Catalytic oxidation of naphthalene using a Pt/Al_2O_3 catalyst. Applied Catalysis B: Environmental, 58, 289-297.

Thammachart, M., Meeyoo, V., Risksomboon, T., Osuwan, S. (2001) Catalytic activity of CeO_2-ZrO_2 mixed oxide catalysts prepared via sol-gel technique: CO oxidation. Catalysis Today, 68, 53-61.

Trimm, D.L., Irshad, M. (1970) The influence of electron directing effects on the catalytic oxidation of toluenes and xylenes. Journal of Catalysis, 18, 142-153.

Weisz, P.B., Prater, C.D. (1954) Interpretation of measurements in experimental catalysis. Advances in Catalysis, 6, 143-196.

Young, G.W., Greene, H.L. (1977) Kinetic modeling for the catalytic oxidation of benzo(a)pyrene. Journal of Catalysis, 50, 258-267.

Zhang, X.-W., Shen, S.-C., Yu, L.E., Kawi, S., Hidajat, K., Simon Ng, K.Y. (2003) Oxidative decomposition of naphthalene by supported metal catalysts. Applied Catalysis A: General, 250, 341-352.